ADVANCING EARTH AND SPACE SCIENCE

JGR Oceans

RESEARCH ARTICLE
10.1029/2021JC017687

Key Points:

- Multimodel wave simulations project a hemispheric contrast in future wave power with a Southern increase versus a Northern decrease
- Wave height change plays a dominant role in shaping wave power change but wave period change exerts a considerable contribution regionally
- Positive trend of Southern Annual Mode and enhanced Arctic warming are found to shape the hemispheric asymmetry in wave power changes

Supporting Information:

Supporting Information may be found in the online version of this article.

Correspondence to:

S.-K. Min,
skmin@postech.ac.kr

Citation:

Patra, A., Min, S.-K., Son, S.-W., & Yeh, S.-W. (2021). Hemispheric asymmetry in future wave power changes: Seasonality and physical mechanisms. *Journal of Geophysical Research: Oceans*, *126*, e2021JC017687. https://doi.org/10.1029/2021JC017687

Received 16 JUN 2021
Accepted 19 NOV 2021

Hemispheric Asymmetry in Future Wave Power Changes: Seasonality and Physical Mechanisms

Anindita Patra[1], Seung-Ki Min[1,2], Seok-Woo Son[3], and Sang-Wook Yeh[4]

[1]Division of Environmental Science and Engineering, Pohang University of Science and Technology, Pohang, South Korea, [2]Institute for Convergence Research and Education in Advanced Technology, Yonsei University, Incheon, South Korea, [3]School of Earth and Environmental Sciences, Seoul National University, Seoul, South Korea, [4]Department of Marine Science and Convergence Engineering, Hanyang University, ERICA, Ansan, South Korea

Abstract This study inspects the global changes in ocean wave power (WP) by the end of the 21st century, relative to the 1979–2005 period, focusing on seasonality and physical mechanisms. The multimodel ocean wave simulations from WAVEWATCH-III, forced with surface winds simulated by seven different CMIP5 global climate models, are particularly examined. These models robustly show a hemispheric asymmetry in WP changes, that is, a decrease in the Northern Hemisphere but an increase in the tropics and Southern Hemisphere, with large seasonal and regional variations. Individual terms of differential WP, which include wave height and wave period changes, are analyzed to isolate the role of each process. Although wave height changes dominate the overall WP changes, wave period changes also play a comparable role in the Southern Hemisphere extratropics especially in the Indian Ocean sector during austral winter (12%). Wave period increase is strikingly higher in austral winter than summer, resembling swell height changes in the Southern Ocean. Intermodel correlation and composite analyses further indicate that the WP increase in the Southern Hemisphere is closely associated with positive Southern Annular Mode (SAM) trend. On the other hand, the WP decrease in the Northern Hemisphere is robustly related with weakened meridional surface temperature gradient during winter, a consequence of Arctic amplification. As a result, models with higher positive SAM trend and larger Arctic warming project stronger hemispheric asymmetries in WP changes.

Plain Language Summary Ocean surface wave is an important contributor to coastal hazards, and understanding its future condition is fundamental for marine disaster prevention. Many studies have focused on wave height changes but wave power, which better characterizes global wave condition than wave height alone, has received less attention. Our projection results, based on recent wave model simulations forced by several global climate models, reveal a distinct hemispheric contrast in wave power changes; an increase in the Southern Hemisphere and a decrease in the Northern Hemisphere. Further analysis of relative contributions of wave height and wave period changes identifies noticeable seasonal and regional characteristics. Although the contribution of wave height changes is dominant across seasons, wave period changes exert an important contribution over Southern Hemisphere extratropics during austral winter. Wind-sea and swell heights exhibit similar pattern changes to those of wave height and period, respectively, supporting their close connections. Robust trend in the Southern Annual Mode toward a more positive phase is found to drive the wave power increase in Southern Hemisphere, irrespective of seasons, while the weakened meridional temperature gradient during winter, as a result of Arctic warming, is important to determine reduced wave activity over Northern Hemisphere.

1. Introduction

To reduce the dependency on fossil fuels and mitigate the related climate change disasters, renewable energies are experiencing rapid interest, financial investment, and technological development. Alongside of other leading renewable energies, ocean wave energy (hereafter simply referred to as wave energy unless otherwise stated) is also promising owing to its additional advantages such as high energy density compared to others, high predictability, low visibility and environmental impact, coastal protection, etc. (Kamranzad & Hadadpour, 2020). The design parameters of wave energy farms depend on wave energy resource variability. Being a key element of climate system (Hemer et al., 2012), waves are likely to be affected by global climate change. Previous studies have claimed that in addition to amount of energy and its seasonality, long-term change is also prerequisite for planning a pilot project (Kamranzad et al., 2021). Therefore, future changes in wave energy resource assessment are crucial for financial and engineering management of wave energy farms.

Wave power (WP), the transport of energy by ocean surface waves, is mainly a function of wave height and period, thus more useful than wave height alone for characterizing the coastal vulnerability. For instance, longer period waves produce higher wave runup and transport greater suspended sediment concentration (Bromirski et al., 2013; Sierra & Casas-Prat, 2014). The changes in wave height and period together impact coastal processes like overtopping discharge, beach flooding, siltation, long-shore sediment transport, etc. (Sierra & Casas-Prat, 2014). As a proxy for coastal flooding and erosion, studying the future changes of WP is necessary, which potentially characterizes the long-term behavior of the global wave conditions better than wave height.

There are many global studies available on wave height projections by the end of 21st century (Fan et al., 2014; Lobeto et al., 2021; Meucci et al., 2020; Morim et al., 2019; O'Grady et al., 2021; Wang et al., 2014), but similar assessments on WP are still limited. In this context, Reguero et al. (2019) reported recent increase in global WP as a consequence of sea surface temperature warming. The regional projected changes in WP can be associated with changes in large-scale atmospheric circulations. Extreme coastal wave energy flux changes in the 21st century are reported in Mentaschi et al. (2017) who also showed their correlation with several climate variability indices.

The present study conducts a comprehensive assessment of future changes in WP and its components (wave height, wave period, wind-sea, and swells) with special attention put on hemispheric and seasonal variations. The study provides new insights into 21st century changes in global wave condition in different fronts. First, a hemispheric asymmetry is demonstrated in future projections of seasonal wave condition using historical and future (based on the Representative Concentration Pathways—RCP8.5 scenario) wave data, produced using WAVEWATCH-III wave model, forced with an ensemble of seven global climate models (GCM) from the Coupled Model Intercomparison Project Phase 5 (CMIP5). Second, we investigate future projections in different terms of differential WP and separate contribution from wind-sea and swell heights. Moreover, separate mechanisms for two hemispheres changes are examined, which control the surface wind change patterns in the extratropics of each hemisphere. Specifically, we consider future changes in the Southern Annual Mode (SAM) and the meridional surface temperature gradient (MTG) in the Northern extratropics focusing on winter seasons. We select SAM and MTG as major drivers of WP changes since they show robust changes in the future with high intermodel agreement. Several studies showed that climate variability modes like North Atlantic Oscillation (NAO) can affect historical changes in regional WP (e.g., Bromirski & Cayan, 2015; Bromirski et al., 2005; Yang & Oh, 2020). However, various well-known climate variability modes such as Arctic Oscillation (AO), NAO, El-Niño-Southern Oscillation (ENSO), Pacific North America pattern (PNA), etc. exhibit uncertain trends in the future with multimodel mean projected changes smaller than the intermodel spreads (Christensen et al., 2013). One exception is the SAM, for which all CMIP5 models exhibit consistent intensification toward its positive phase at the late 21st century. Third, in contrast with coastal area-average changes in mechanism studies (Mentaschi et al., 2017), we discuss spatial change patterns over global ocean through intermodel correlation and composite analysis. Besides coastal impact, open ocean swell changes can have remarkable influences on marine atmospheric boundary layer (Semedo et al., 2009; Smedman et al., 1999; Sullivan et al., 2008) through changing vertical wind profile and turbulence structure with repercussions in lower atmosphere stability (Lemos et al., 2021).

It is noteworthy that Karnauskas et al. (2018) described distinct mechanism in each hemisphere for the late 21st century changes in continental wind power. Their study accounted Arctic amplification for wind power decrease across Northern Hemisphere midlatitude lands; and enhanced land-sea thermal gradient for the increase over land areas across tropics and Southern subtropics. Here we explore hemisphere-specific physical mechanisms for ocean WP changes through more detailed analyses.

2. Data and Methods

2.1. Model Data

The study uses ocean wave data from historical and RCP8.5 scenario simulations produced by the global ocean wave model WAVEWATCH-III (WWIII v.3.14). The data are taken from the CSIRO data server [Collaboration for Australian Weather and Climate Research (CAWCR) data set available at https://doi.org/10.4225/08/55C991CC3F0E8]. The WWIII model, implemented at $1° \times 1°$ resolution, was forced with surface wind and sea ice area fraction from different CMIP5 GCMs (Hemer & Trenham, 2016). Here, a total of seven

Table 1
List of CMIP5 Models and Their Horizontal Resolutions and Equilibrium Climate Sensitivity (ECS) Values

			SAM (DJF)		SAM (JJA)		MTG (DJF)	
Model	Resolution (longitude° × latitude°)	ECS (°C)	Strong	Weak	Strong	Weak	Strong	Weak
ACCESS1.0	1.88 × 1.25	3.8	×					
BCC-CSM1.1	2.8 × 2.8	2.8		×		×		×
GFDL-CM3	2.5 × 2.0	4.0	×		×		×	
HadGEM2-ES	1.88 × 1.25	4.6	×				×	
INMCM4	2.0 × 1.25	2.1		×				×
MIROC5	1.4 × 1.4	2.7	×		×			
MRI-CGCM3	1.1 × 1.1	2.6		×		×		×

Note. Models selected for stronger and weaker future changes in the intensified SAM (toward its positive phase) for DJF and JJA and the reduced meridional temperature gradient in NH (MTG) for DJF are denoted.

WWIII model runs are selected, driven by different GCMs: ACCESS1.0, BCC-CSM1.1, GFDL-CM3, HadGEM2-ES, INMCM4, MIROC5, and MRI-CGCM3 (Table 1). These seven models are a subset of COWCLIP 2.0 and have been chosen based on the 6-hourly data availability over the full analysis period. COWCLIP 2.0 data set comprises wave parameters at monthly, seasonal, and annual resolution from seven different clusters (Morim et al., 2020), which are available at http://thredds.aodn.org.au/thredds/catalog/CSIRO/Climatology/COWCLIP2/catalog.html. Although intercluster differences need to be considered as an important source for future projection uncertainties (Morim et al., 2020), the present group of models broadly represents the larger ensemble, in terms of mean and 99th percentile as well as 21st century projected changes (Meucci et al., 2020). In addition, the selected models were assessed as best performers in Hemer and Trenham (2016), who evaluated the model simulated climatological wave parameters (significant wave height, maximum wave height, mean wave period, and direction) against three different reanalysis datasets over 13 subregions of the global ocean. The integrated wave parameters are obtained from the 6-hourly archives for the historical (1979–2005) and future (2081–2099) periods, only during which data are available. Seasonal means are calculated from 6-hourly data during DJF (December to February) and JJA (June to August). Finally, differences in long-term averages between future and historical period are analyzed, assuming linear changes responding to future global warming levels. Projection results remain unaffected when using the common 19 years for historical (1987–2005) and future period (not shown).

To understand driving mechanisms for extratropical surface wind changes across models, the present study also considered monthly sea level pressure (SLP) and surface air temperature fields from the seven CMIP5 models for both historical and RCP8.5 scenario simulations. In addition, to further check the influence of global warming intensity on intermodel differences in WP projections, equilibrium climate sensitivity (ECS) values for these models are analyzed, which are obtained from Meehl et al. (2020). ECS is an estimate of the eventual steady state global warming at double CO_2 (Table 1).

2.2. Analysis Methods

The WP can be defined as

$$\mathrm{WP} = \frac{\rho g^2}{64\pi} H_s^{\,2}\ T_e$$

where ρ is water density, g is gravitational acceleration, H_s is significant wave height, and T_e is energy period. The wave power for an irregular sea-state is defined using T_e (Dean & Dalrymple, 1991; Reguero et al., 2015, 2019; Sheng & Li, 2017; Tucker & Pitt, 2001). However, T_e is usually not specified but estimated from other parameters. Following previous studies (Reguero et al., 2015), we estimate T_e from mean wave period (T_m) through the empirical relationship: $T_e = 0.538 \times T_m$, which is equivalent to peak enhancement mean factor of 3.3 in a JONSWAP spectrum. By using T_m, WP can be expressed as follows:

$$\mathrm{WP} \;= cH_s{}^2T_m \quad c = 0.538\times\frac{\rho g^2}{64\pi} = 0.256 \tag{1}$$

Here, we consider differential WP to calculate future changes (difference between 2081–2099 and 1979–2005) in different terms of differential WP as

$$\overline{\mathrm{WP}} + \Delta\mathrm{WP} = c(\overline{H}+h)^2(\overline{T}+t)$$

where ΔWP, h and t is future changes in WP, wave height and wave period, respectively; and $\overline{\mathrm{WP}}$, $\overline{H}$, $\overline{T}$ are their climatological values in the present period (1979–2005). Note that we omit subscript s and m for brevity. The above equation can be expanded as

$$c\overline{H}^2\overline{T} \;+\; \Delta\mathrm{WP} = c[\overline{H}^2\overline{T} \;+\; 2\overline{H}h\overline{T} \;+\; h^2\overline{T} \;+\; \overline{H}^2t \;+\; 2\overline{H}ht \;+\; h^2t]$$

$$\Delta\mathrm{WP} = c[2\overline{H}h\overline{T} + \overline{H}^2t + 2\overline{H}ht + h^2\overline{T} + h^2t] \tag{2}$$

These five terms in right-hand side are calculated to estimate contribution from wave height and/or wave period, separately. The first and second term on the r.h.s of Equation 2 can be interpreted as major individual contribution from future changes in wave height and wave period, respectively. The last three nonlinear terms (second-order or third-order change) are combinations of changes in height and period so generally have relatively small amplitudes. The climatology factors like $2c\overline{H}\;\overline{T}$ and $c\overline{H}^2$ in the first and second term play a role in converting individual future changes in wave height and wave period (h and t, respectively) into WP unit, enabling a quantitative comparison of their contributions.

Relation between wind-sea height (H_w), swell height (H_{Sw}), and total wave height (H) is as follows:

$$H^2 = H_w{}^2 + H_{Sw}{}^2 \tag{3}$$

Similar to WP, differential terms of wave height can be introduced by considering future changes in wind-sea height (h_w) and swell height (h_{Sw}):

$$(\overline{H}+h)^2 = (\overline{H_w}+h_w)^2 + (\overline{H_{Sw}}+h_{Sw})^2$$

$$2\overline{H}h + h^2 = 2\overline{H_w}h_w + 2\overline{H_{Sw}}h_{Sw} + h_w{}^2 + h_{Sw}{}^2$$

Ignoring small nonlinear terms, we obtain below equation:

$$2\overline{H}h \;\approx 2\overline{H_w}h_w + 2\overline{H_{Sw}}h_{Sw} \tag{4}$$

where the two terms in r.h.s imply relative contribution from wind-sea and swell height, respectively. Although the peak wave period (T_p) is known as a better measure for swells than T_m, T_p can be noisy for cases where there is a mixture of swell and wind-sea (Young, 1999). Nevertheless, to check the sensitivity of our results, we have repeated our analysis using T_p through its empirical relationship with T_e (= 0.857 × T_p) following Hemer et al. (2017) and obtained similar results (see below).

To analyze physical mechanisms shaping the future WP patterns, the indices for Southern Annular mode (SAM) and Northern Hemisphere (NH) meridional surface air temperature gradient (MTG) are calculated from same seven CMIP5 models. The SAM index is defined as difference in normalized monthly zonal mean SLPs between 40°S and 65°S (Gong & Wang, 1999; Son et al., 2021). Further, the seasonal-mean SAM index is standardized by subtracting the seasonal mean and then dividing it by the seasonal standard deviation over reference period, as done in Patra et al. (2021). The NH winter MTG is estimated as the absolute value of the surface air temperature difference between high (65°–85°N) and low (20°–40°N) latitudes in CMIP5 models, reduction of which represents Arctic amplification (e.g., Chemke & Polvani, 2020).

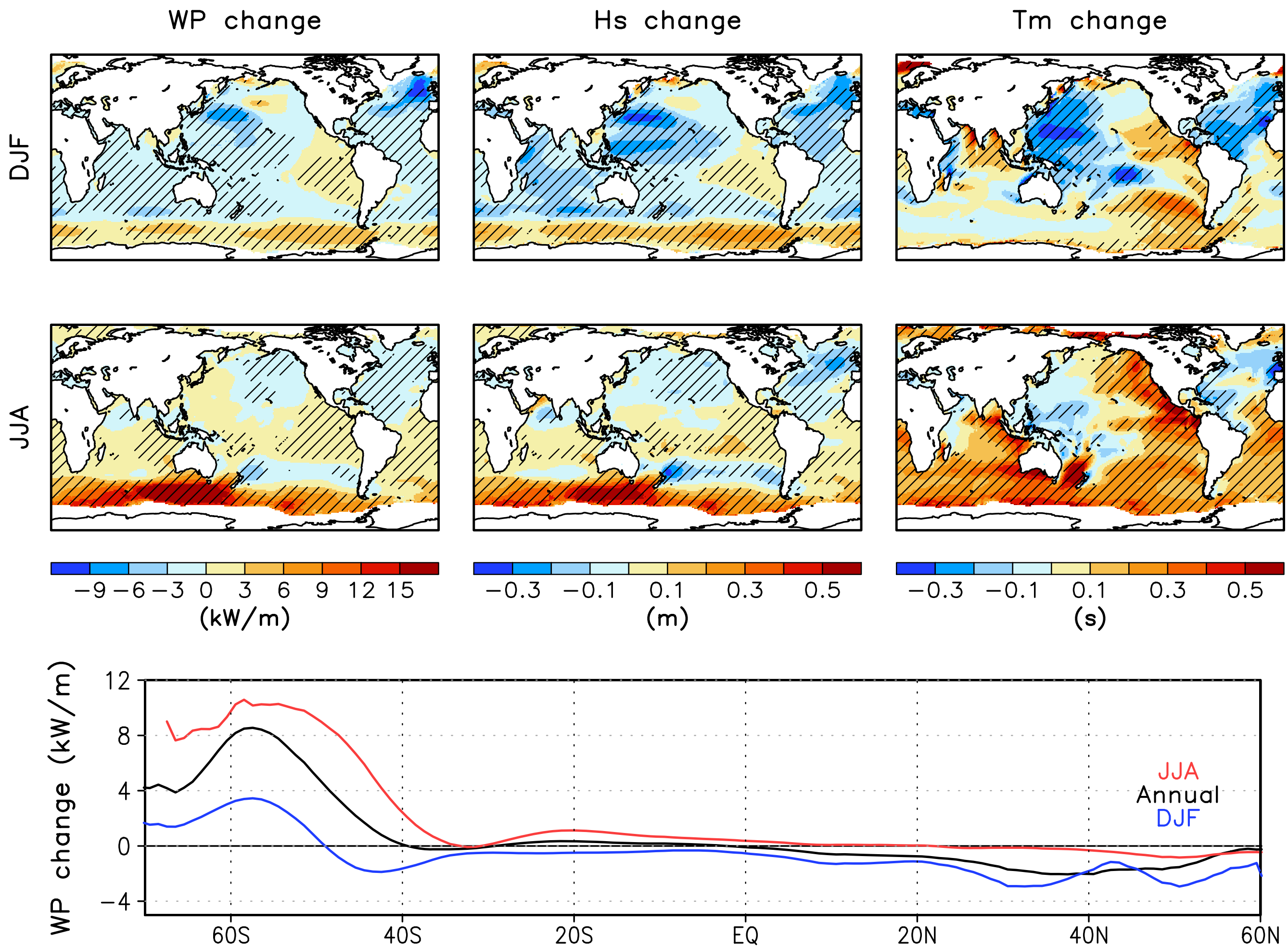

Figure 1. (Upper panel) Multimodel mean projected changes in wave power (WP), significant wave height (H_s), and mean wave period (T_m) during 2081–2099 relative to 1979–2005 for DJF (upper) and JJA (middle). Hatchings represent significant change at 10% level according to a paired *t* test. (Lower panel) Zonal mean of WP changes for annual and seasonal means (DJF and JJA).

3. Results

3.1. Global WP Change Patterns

Figure 1 shows multimodel mean projected changes in WP during the late 21st century under the RCP 8.5 scenario, which reflect strong interhemispheric asymmetries. Significant increases in WP are generally projected across tropical and Southern Hemisphere (SH) high-latitude regions, while reductions are projected broadly across the NH extratropical regions. Strong seasonal variation exists in future changes, especially in the tropics and NH. On the other hand, in the SH high-latitudes, consistent increase is observed across seasonal evolution. In JJA, robust (in terms of intermodel agreement) increases are found over the whole SH except small regions over subtropical Pacific. In DJF, robust increases are seen in limited areas in the NH. Projection results based on percentage change (relative to historical magnitude) show similar patterns (figure not shown). Although spatial patterns in WP projections are similar to wave height change patterns, contributions of wave period also count. Strong hemispheric and seasonal variabilities are projected for multimodel mean changes in wave period. In JJA, robust increase in wave period is projected across models for nearly whole global ocean except areas over northwestern Pacific and North Atlantic. These areas are projected to have reduced (robust) wave period during DJF. We quantify relative contributions of wave height and period changes to the total WP below.

Zonal average changes (Figure 1, bottom panel) evidently show asymmetric dependence on hemisphere with substantial seasonality. In case of annual mean WP, projected increase is seen for SH and decrease for NH.

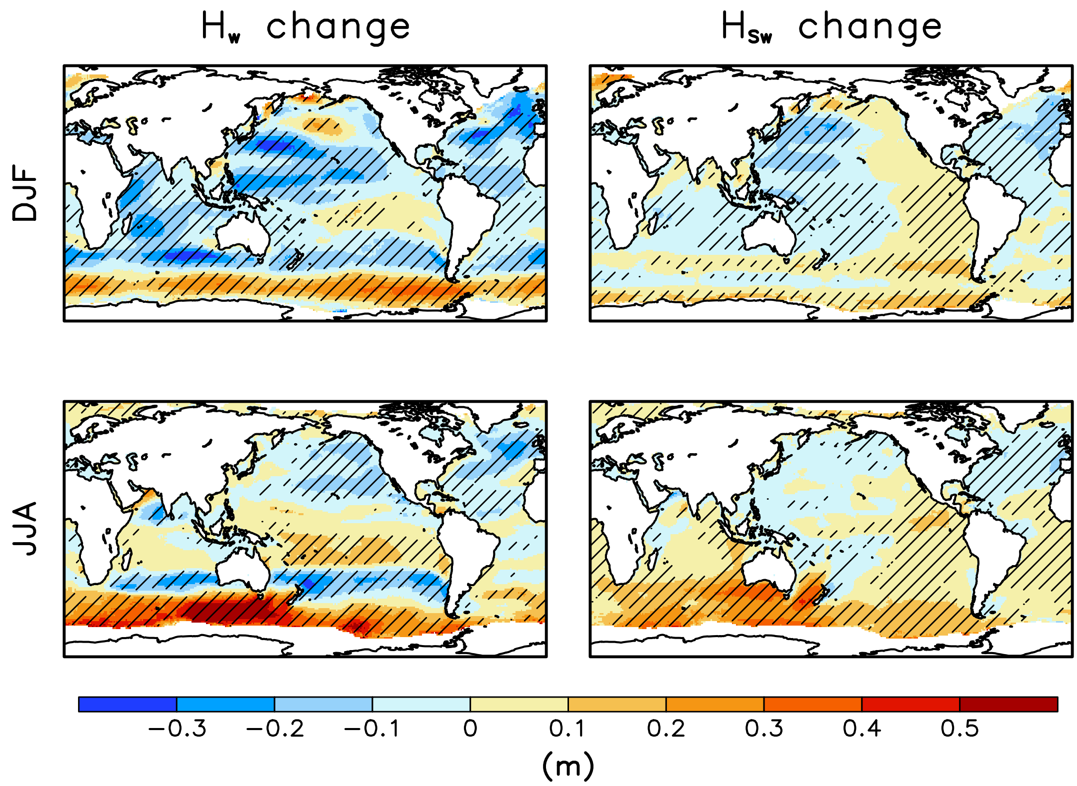

Figure 2. Multimodel mean projected changes in significant wave height from wind-seas (H_w) and from swells (H_{Sw}) during 2081–2099 relative to 1979–2005 for DJF (upper) and JJA (lower).

During DJF, zonal averaged increase is observed only in the SH high-latitudes. In comparison, strong increase is projected over SH and relatively less reduction over NH during JJA. These responses are generally consistent with wind power projections over the land areas by Karnauskas et al. (2018), who found increases in wind power over tropics and southern subtropics and decreases over NH midlatitude lands.

Seasonal variations in wind-sea and swell height changes are presented in Figure 2. Although wind-sea height has a larger contribution to the total wave height changes, the influence of increased swell height is still prominent in the SH. The robust projected decrease in the SH midlatitudes is found for wind-sea height change in JJA but is limited to a small region in Pacific for total wave height change (Figure 1, JJA), which is due to the influence of intensified swells. Seasonal variations in swell height changes are contrasting between DJF and JJA, with a striking resemblance with the wave period change patterns (compare right columns of Figures 1 and 2). Intermodel correlation between swell height change and wave period change shows significantly high correlation (>0.8) almost all over the global ocean as well as in zonally averaged projected changes (around 0.9) for both seasons (Figure S1 in Supporting Information S1), indicating their close association. Note that the projected increases in wind-seas, swells, total wave height, wave period, and WP are strongest over SH high-latitudes, where land fraction is almost zero (Amores & Marcos, 2020).

Multimodel mean future changes in the first three terms of differential WP (Equation 2) are compared in order to quantify their relative contribution to the total WP changes (Figure 3). The first term associated with wave height change (2c $\overline{H}h\overline{T}$) is the dominating term followed by the second term associate with wave period change (c$\overline{H}^2 t$), with both terms showing seasonal and regional dependence. The third term exhibits very small changes. The fourth and fifth terms are very small in magnitude (not shown). As expected, spatial patterns of the first and second terms resemble those of wave height and period changes, respectively (Figure 1). The contribution of wave period changes is prominent over the Southern Ocean between 45°S and 60°S during JJA (note the different shading intervals). In addition, it is strongest over the Indian Ocean sector and contributes around 12% (based on area averaged values over 80–170°E, 40–60°S) to the total WP changes. Indeed, when analyzing JJA climatology of wave energy flux vectors, which are defined using zonal and meridional component as cosine and sine of peak

10.1029/2021JC017687

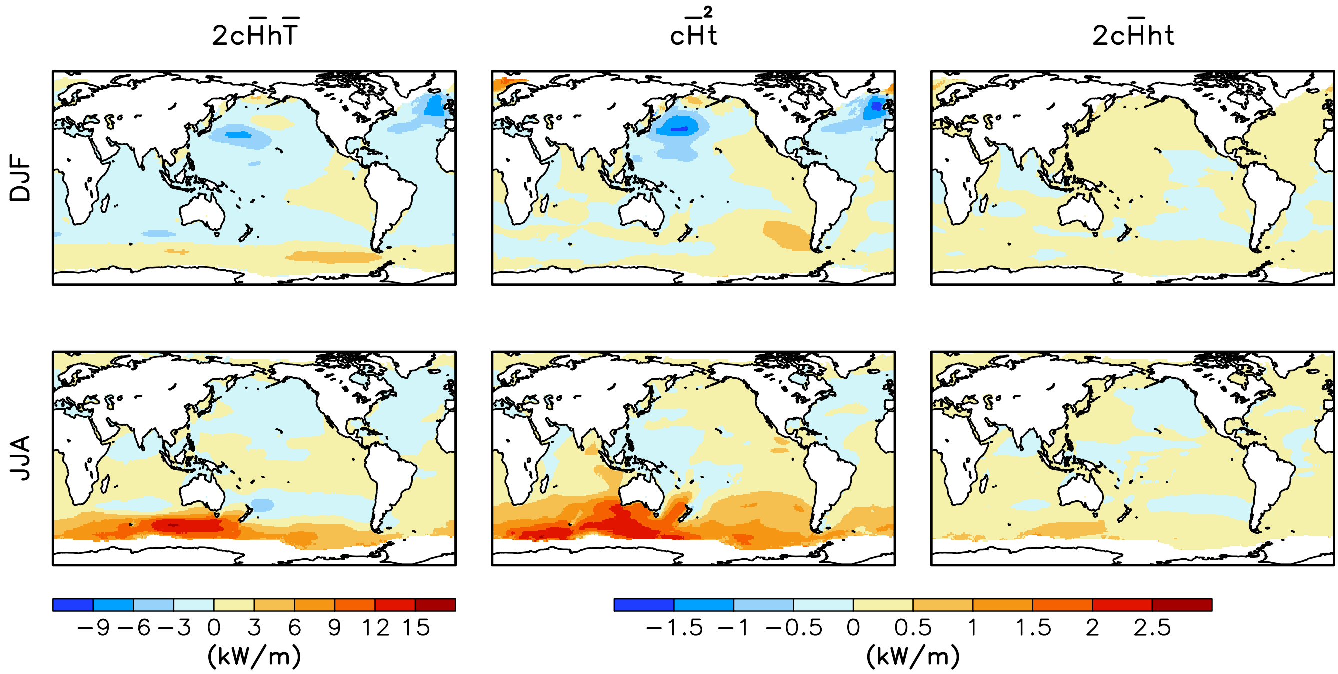

Figure 3. Multimodel mean changes in different terms of differential WP in 2081–2099 relative to 1979–2005 based on the first three terms of r.h.s of Equation 2. Note the different shading intervals for the first term and the second and third terms.

wave direction and WP as magnitude of the vectors (Marshall et al., 2018), strongest wave energy fluxes are observed over the Indian Ocean sector of Southern Ocean (figure not shown). Concerning the NH, these terms add to decrease over North Pacific and North Atlantic during DJF, which is consistent with previous studies projecting decreased swell events in the NH swell generation areas (Amores & Marcos, 2020).

Likewise, we calculated wind-sea and swell height contributions to total wave height change based on Equation 4. Figure 4 shows spatial patterns of wind-sea and swell height changes where $2c\overline{T}$ has been multiplied to obtain corresponding contributions of wind-sea height and swell height changes to the total WP change (refer to Equation 2). As expected, the wind-sea height term ($2c\overline{H_w}h_w\overline{T}$) has a larger contribution than the swell height term ($2c\overline{H_{Sw}}h_{Sw}\overline{T}$), mostly explaining the total change ($2c\overline{H}h\overline{T}$, see Figure 3), confirming the dominant influence of wind-sea height. A substantial contribution of swell height change is found over swell dominated regions in JJA (note the different shading interval), especially in the Indian Ocean sector of Southern Ocean (80°–170°E, 40°–60°S). A quantification using area averaged change over the region confirms a considerable contribution of swell height, explaining around 21% of the total WP changes, compared to 64% by the wind-sea height contribution.

As the peak wave period T_p provides a good measure of the long period swell regionally (Young, 1999), this analysis has been repeated using T_p instead of T_m (see above for details). The T_p-based results (Figure S2 in Supporting Information S1) agree well with the T_m-based results (Figure 4) with only slight differences in magnitudes. Also, future changes in T_p and WP computed using T_p (Figure S3 in Supporting Information S1) exhibit similar patterns to the T_m-based ones (Figure 1), reaffirming the interhemispheric and seasonal features. Interestingly, the swell height change pattern bears a stronger resemblance to the T_m change pattern than the T_p change pattern, which might be due to the presence of mixed sea states as discussed above. Generally higher intermodel correlations between swell height and T_m changes also supports this (compare Figures S4 and S1 in Supporting Information S1).

3.2. Mechanisms Behind Projected WP Changes

The following section examines the possible mechanisms for the hemispheric asymmetry in WP changes focusing on SAM and MTG influences as discussed above. For explaining the changes in SH, relation with SAM changes in the late 21st century is assessed, which is known to have a strong influence on storms and extreme winds and

10.1029/2021JC017687

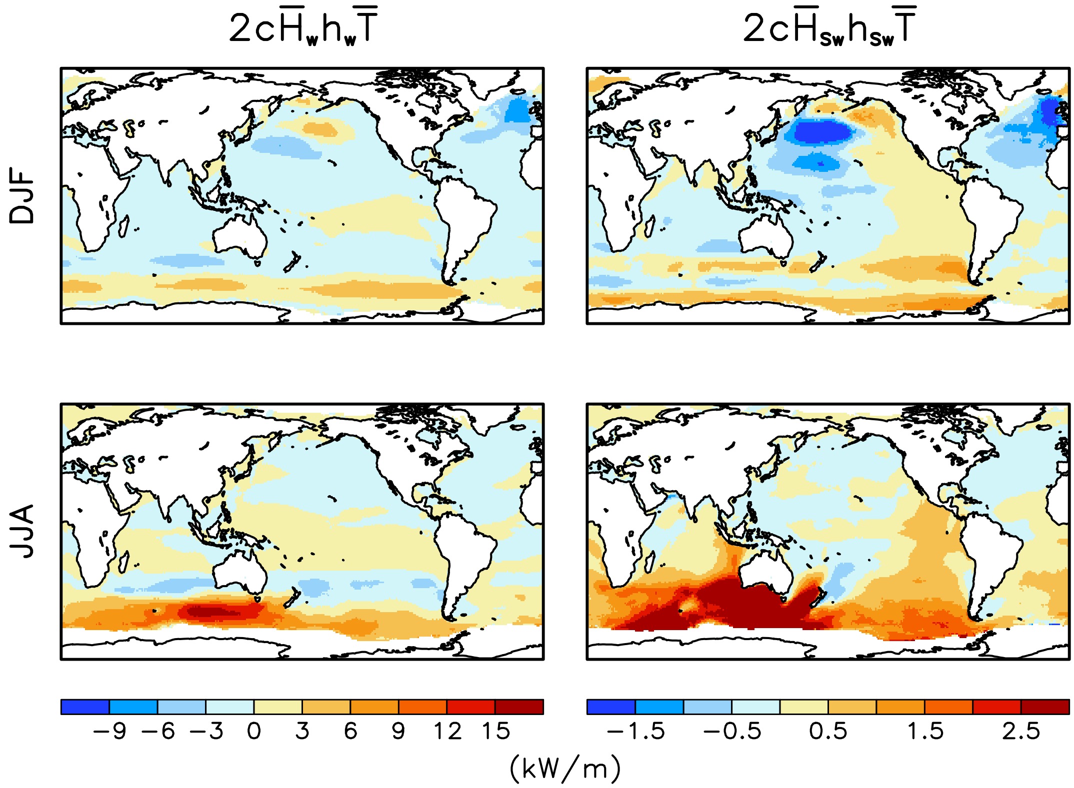

Figure 4. Relative contribution of wind-sea (left) and swell heights (right) to total wave power changes in 2081–2099 relative to 1979–2005 based on r.h.s of Equation 4. Note $2c\overline{T}$ has been multiplied to obtain corresponding contributions to the total WP change (refer to Equation 2).

thereby wave height changes (e.g., Mentaschi et al., 2017; Patra et al., 2020). All the models (except one in DJF) and their multimodel means project intensified SAM toward its positive phase in the future for both seasons, although comparably higher in JJA (Figure 5, low panel). The intermodel correlation between WP and SAM changes (Figure 5, upper panel) is highly positive and robust across the Southern Ocean and tropics of SH in JJA, while it is limited to the Southern Ocean (with reduced longitudinal coverage) in DJF. Almost same patterns of intermodel correlation are obtained with wave height changes. However, wave period change exhibits different correlation patterns from those for WP and height changes. During austral winter, positive correlation is seen over the entire eastern Pacific, which confirms crossing of the SH swells to the NH. Eastward-propagating swells have much influence on the eastern side of the Pacific and Indian basin. In contrast, this correlation is limited to the eastern Pacific region of Southern Ocean in boreal winter. As expected, wind-sea height change has similar correlation patterns to those for total wave height change, whereas swell height change has similarity to the wave period case (figure not shown). It is interesting to see that the intermodel correlation with SAM bears a striking resemblance to absolute future change pattern in all the parameters (Figure 1), especially in SH. Further, SAM shows highly robust negative correlation with WP over North Pacific and North Atlantic. This seems to be partly associated with global warming which drives both SAM (toward positive phase) and NH WP changes (toward decreases, see below) in these CMIP5 models. Indeed, positive intermodel correlations between equilibrium climate sensitivity (ECS, Table 1) and future SAM indicates that models with stronger global warming tend to project a stronger SAM (Figure S5 in Supporting Information S1). In addition, the intermodel correlation pattern of SAM changes with the first and second terms (r.h.s of Equation 2) of WP changes is similar with that of wave height and period changes, respectively (figure not shown).

To further check the SAM influences on WP, we carried out composite analysis of WP changes for stronger and weaker SAM change models (Figures S6 and S7 in Supporting Information S1). Models selected for stronger and weaker SAM group are listed in Table 1. Despite small sample size, the overall results are consistent with the correlation analysis shown in Figure 5. Models with higher SAM intensification have stronger WP increase in the

10.1029/2021JC017687

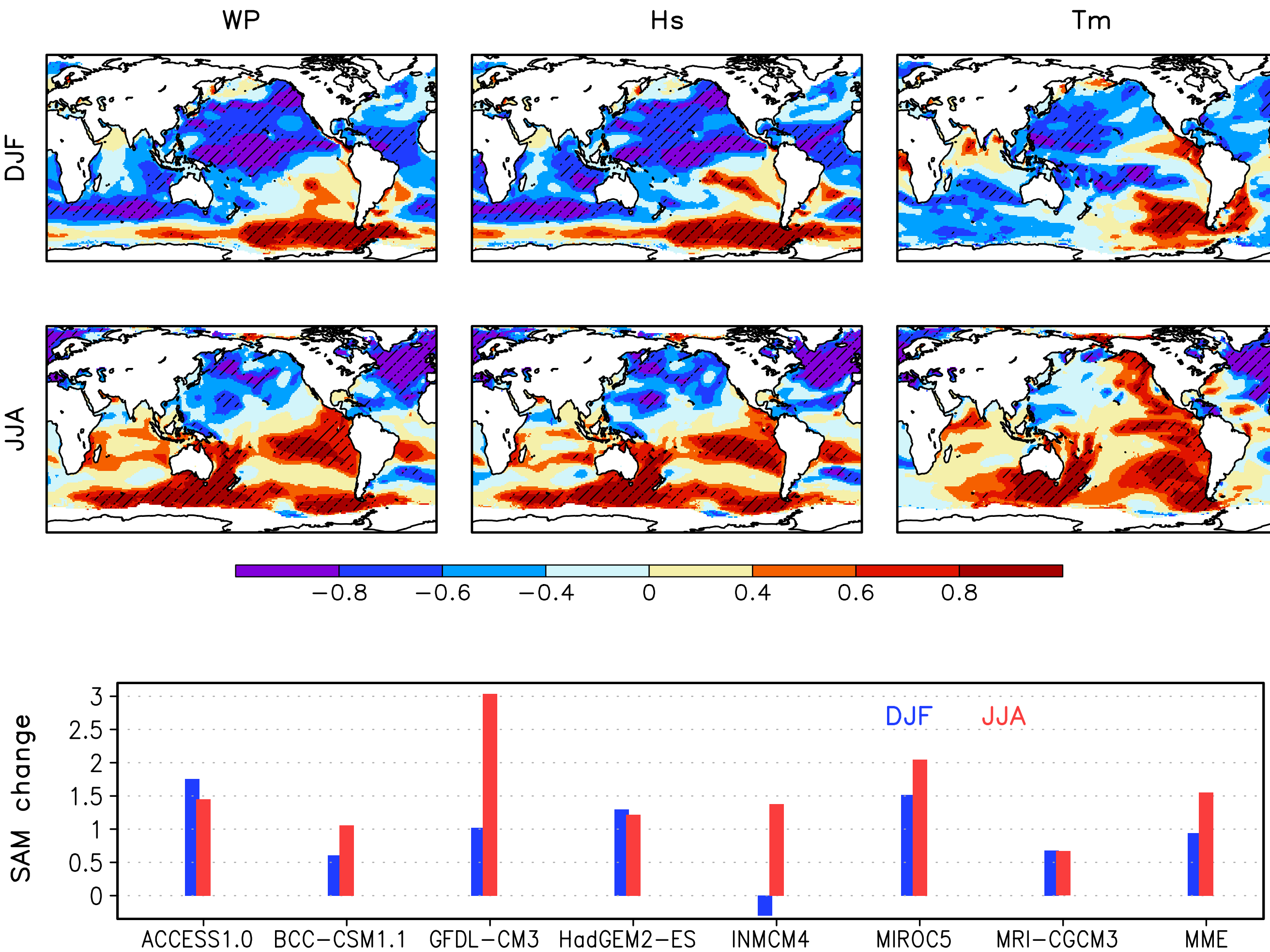

Figure 5. Spatial distributions of intermodel correlation between the projected changes in WP, H_s, and T_m and the SAM changes during 2081–2099 relative to 1979–2005 for DJF (upper) and JJA (middle). Hatchings indicate grids having significant correlation coefficient at 10% level. (Lower panel) Future changes in SAM for each model and multimodel ensemble mean (MME).

Southern Ocean and tropics in JJA (Figure S7 in Supporting Information S1). In DJF, higher SAM models shows greater WP increase over the Southern Ocean and greater decrease over the northeastern Pacific and westernmost north Atlantic relative to lower SAM models (Figure S6 in Supporting Information S1). Interestingly, the areas with greater decreases have larger intermodel spread, due to great discrepancies between models, consistent with previous studies (Lobeto et al., 2021, their Figure 3). In a similar way, models with higher SAM change tend to simulate larger intensification of swells originating from the Southern Ocean, particularly on the eastern side of South Indian and South Pacific Oceans. Evidently, composite patterns of wind-sea change are quite similar to those of WP.

Besides the SAM, intensification of southeasterly trades contributes to the WP intensification over SH tropics with remarkable seasonality (Figure S8 in Supporting Information S1). In JJA, it covers full tropical band in SH whereas it is only seen for Pacific in DJF. Notable is a wedge-shaped increasing pattern in wind speed (over tropical Pacific in SH) as well as in wind-sea height (Figure 2) during DJF. A hemispheric asymmetry is clearly evident from the zonal mean pattern of future wind speed change. Not only the mean, interannual variability of WP also shows significant changes in future climate (Figure S9 in Supporting Information S1). Special attention should be given to the southwestern coast of Australia; as the eastern South Indian Ocean is projected to undergo significant increases in the interannual WP variability by the end of 21st century. This implies that along with mean of the distribution, year-to-year fluctuations also increase and that makes the tail of the WP distribution

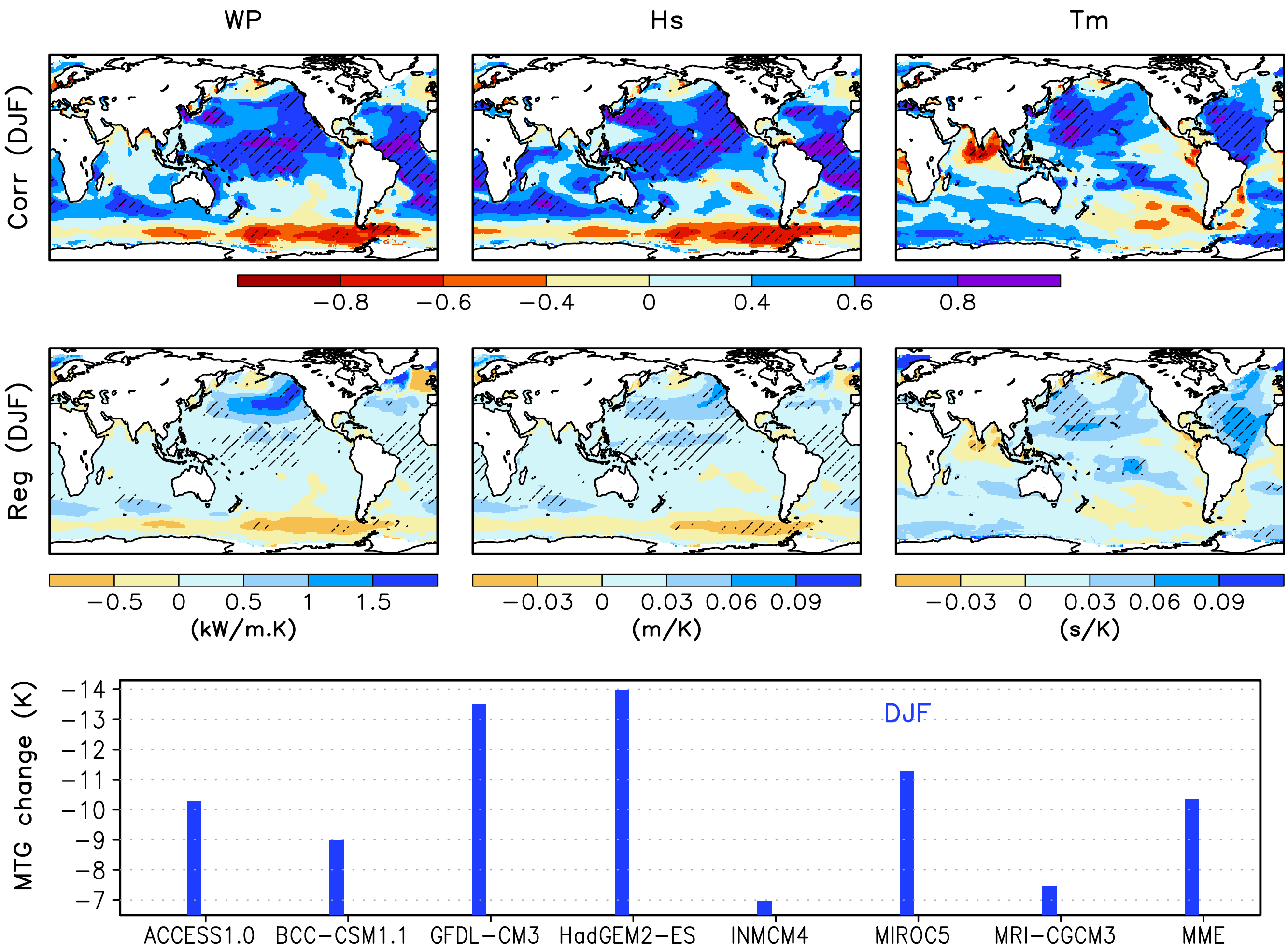

Figure 6. Spatial distributions of intermodel correlation and regression between the projected changes in WP, H_s, and T_m and the changes in meridional temperature gradient over NH (MTG) for DJF. Hatching indicates significance at 10% level. (Lower panel) Future changes in MTG for each model and multimodel ensemble mean (MME).

heavier and consequently stronger extremes. An interesting fact is that the intermodel correlation between SAM change and interannual standard deviation change in WP is significantly positive over this region.

To explain the NH decrease in WP, we consider future changes in the meridional gradient of surface air temperature (MTG). In the NH, polar amplification acts to reduce the meridional temperature gradient, which causes general weakening and poleward shift of the storm tracks during winter (Barnes & Polvani, 2013; Chang et al., 2012; Harvey et al., 2014). Regarding intermodel differences, the midlatitude jet tends to be shifted relatively equatorward in models with strong Arctic surface warming (Yim et al., 2016). A strong reduction in MTG due to Arctic warming is projected by all the seven models during DJF (Figure 6) with very high (−0.97) intermodel correlation between the MTG and Arctic surface warming. Spatial distribution of the intermodel correlation between WP and MTG changes shows significantly positive correlation over NH tropics to extratropics. That implies that WP decreases strongly follow the reduction in MTG or Arctic amplification. Similar conclusion can be drawn for wave height and period changes. Additionally, intermodel linear regression of WP changes onto MTG change exhibit large positive values over NH. It is noteworthy to mention a strong intermodel correlation between MTG change and ECS (Figure S5 in Supporting Information S1), which indicates a stronger WP decrease in NH under higher global warming levels.

In the same way as done for SAM, we carried out a composite analysis for stronger and weaker change model groups for MTG (see Table 1). Overall, models with higher MTG reduction (i.e., stronger Arctic warming) have stronger decreases in WP and wind-sea and swell heights over NH (Figure S10 in Supporting Information S1).

On the other hand, models having lower MTG reduction shows much weaker changes in WP overall. It is notable that composite differences are rather uncertain due to the limited number of models used (Table 1). Nevertheless, when checking the intermodel correlation between climatology and projection, the present-day mean conditions of WP and its components are not clearly linked with corresponding future responses to greenhouse warming. Further investigation using more models is warranted to better identify uncertainty factors in WP projections.

4. Summary and Conclusions

The study investigates global changes in WP in the late 21st century using an ensemble of WAVEWATCH-III wave projections forced by seven different CMIP5 models. We provide a detailed analysis of the seasonal differences between Southern and Northern Hemisphere changes in future climate as well as explore physical mechanisms for such changes. This is the first study demonstrating the hemispheric asymmetry in future WP projections with relative contributions of wind-sea and swell heights quantified. Moreover, physical mechanisms for the hemispheric changes are examined, focusing on the two drivers of SAM and MTG which exhibit robust future changes.

It is shown that there is a strong asymmetry between the hemispheres in the simulated WP changes responding to anthropogenic radiative forcing. This asymmetry exists across seasons and also in the annual mean. By the end of 21st century, multimodel mean under RCP8.5 scenarios projects a decrease in WP over NH extratropical ocean and an increase overtropics and SH high-latitudes, with notable seasonal variability. The spatial patterns of WP changes resemble those of wave height, particularly wind-sea height, although noticeable differences are present among them. In a similar way, future changes in wave period and swell height have spatial resemblance. Eastward-propagating swells generated in Southern Ocean are projected to intensify almost everywhere in JJA, with stronger magnitudes along the western coasts. In contrast, swells developed in NH are projected to weaken, particularly in DJF. It is found that the incremental change in WP is driven by highest contribution from incremental change in wave height and second highest from change in wave period. Interestingly, influence of wave period change is significant over the Southern Ocean, distinctly in JJA, due to enhanced swell impacts. Likewise, swell contribution to incremental WP changes is remarkable over that region.

Future amplification of the positive SAM, consistent with the poleward shift of SH jets, is found to drive future WP increases across SH, during both austral winter and summer. Intensification of both wave height and period due to the SAM change implies multifold increases in WP. On the other hand, CMIP5 models project a future weakening in NH meridional surface temperature gradient, which acts to reduce NH wave height and period and hence WP. Tropical intensification is assessed to be driven by a remote influence of SAM and also the intensification of trade winds in SH. Interestingly, across CMIP5 models, the extent of future changes in SAM and MTG follows model's equilibrium climate sensitivity (ECS). Thus, in a warmer climate, we expect stronger increase and decrease for SH and NH, respectively, implying larger hemispheric asymmetry. Our detailed assessment of climate change impacts on global WP behaviors will be impactful to coastal vulnerability projection as well as wave energy development plans.

A few caveats remain. It should be noted that although this study focuses on hemispheric scale changes, regional responses will be more important for adaptation and impact assessments. Therefore, the physical mechanism of future wave power changes at regional scales needs to be explored with consideration of the possible influences of relevant climate variability modes such as NAO, ENSO, PNA, etc. In addition, there might be impact of decadal climate variabilities on the intermodel spread depending on their phases, which needs to be investigated in future research.

Data Availability Statement

The authors acknowledge CSIRO for producing CAWCR Global wind-wave 21st century climate projections data set and making freely available (https://doi.org/10.4225/08/55C991CC3F0E8). CMIP5 data are freely downloadable (https://esgf-node.llnl.gov/projects/cmip5/).

Acknowledgments

Authors thank three anonymous reviewers for their constructive comments. This study was supported by National Research Foundation of Korea (NRF) grant funded by the South Korean government (MSIT) (NRF-2018R1A5A1024958).

References

Amores, A., & Marcos, M. (2020). Ocean swells along the global coastlines and their climate projections for the twenty-first century. *Journal of Climate*, *33*, 185–199. https://doi.org/10.1175/JCLI-D-19-0216.1

Barnes, E. A., & Polvani, L. (2013). Response of the midlatitude jets, and of their variability, to increased greenhouse gases in the CMIP5 models. *Journal of Climate*, *26*, 7117–7135. https://doi.org/10.1175/JCLI-D-12-00536.1

Bromirski, P. D., & Cayan, D. R. (2015). Wave power variability and trends across the North Atlantic influenced by decadal climate patterns. *Journal of Geophysical Research: Oceans*, *120*, 3419–3443. https://doi.org/10.1002/2014JC010440

Bromirski, P. D., Cayan, D. R., & Flick, R. E. (2005). Wave spectral energy variability in the northeast Pacific. *Journal of Geophysical Research*, *110*, C30115. https://doi.org/10.1029/2004JC002398

Bromirski, P. D., Cayan, D. R., Helly, J., & Wittmann, P. (2013). Wave power variability and trends across the North Pacific. *Journal of Geophysical Research: Oceans*, *118*, 6329–6348. https://doi.org/10.1002/2013JC009189

Chang, E. K. M., Guo, Y., & Xia, X. (2012). CMIP5 multimodel ensemble projection of storm track change under global warming. *Journal of Geophysical Research*, *117*, D23118. https://doi.org/10.1029/2012JD018578

Chemke, R., & Polvani, L. M. (2020). Linking midlatitudes eddy heat flux trends and polar amplification. *Npj Climate and Atmospheric Science*, *3*, 8. https://doi.org/10.1038/s41612-020-0111-7

Christensen, J. H., Krishna Kumar, K., Aldrian, E., An, S.-I., Cavalcanti, I. F. A., de Castro, M., et al. (2013). Climate phenomena and their relevance for future regional climate change. In *Climate change 2013: The physical science basis. Contribution of working group I to the fifth assessment report of the intergovernmental panel on climate change*. Cambridge University Press.

Dean, R. G., & Dalrymple, R. A. (1991). *Advanced series on ocean engineering: Water wave mechanics for engineers and scientists*. World Scientific.

Fan, Y., Lin, S. J., Griffies, S. M., & Hemer, M. A. (2014). Simulated global swell and wind-sea climate and their responses to anthropogenic climate change at the end of the twenty-first century. *Journal of Climate*, *27*, 3516–3536. https://doi.org/10.1175/JCLI-D-13-00198.1

Gong, D., & Wang, S. (1999). Definition of Antarctic oscillation index. *Geophysical Research Letters*, *40*, 1189–1462. https://doi.org/10.1029/1999GL900003

Harvey, B. J., Shaffrey, L. C., & Woollings, T. J. (2014). Equator-to-pole temperature differences and the extra-tropical storm track responses of the CMIP5 climate models. *Climate Dynamics*, *43*, 1171–1182. https://doi.org/10.1007/s00382-013-1883-9

Hemer, M. A., & Trenham, C. E. (2016). Evaluation of a CMIP5 derived dynamical global wind wave climate model ensemble. *Ocean Modelling*, *103*, 190–203. https://doi.org/10.1016/j.ocemod.2015.10.009

Hemer, M. A., Wang, X. L., Weisssse, R., & Swail, V. R. (2012). Advancing wind-waves climate science: The COWCLIP project. *Bulletin of the American Meteorological Society*, *93*, 791–796. https://doi.org/10.1175/BAMS-D-11-00184.1

Hemer, M. A., Zieger, S., Durrant, T., O'Grady, J., Hoeke, R. K., McInnes, K. L., & Rosebrock, U. (2017). A revised assessment of Australia's national wave energy resource. *Renewable Energy*, *114*, 85–107. https://doi.org/10.1016/j.renene.2016.08.039

Kamranzad, B., & Hadadpour, S. (2020). A multi-criteria approach for selection of wave energy converter/location. *Energy*, *204*, 117924. https://doi.org/10.1016/j.energy.2020.117924

Kamranzad, B., Lin, P., & Iglesias, G. (2021). Combining methodologies on the impact of inter and intra-annual variation of wave energy on selection of suitable location and technology. *Renewable Energy*, *172*, 697–713. https://doi.org/10.1016/j.renene.2021.03.062

Karnauskas, K. B., Lundquist, J. K., & Zhang, L. (2018). Southward shift of the global wind energy resource under high carbon dioxide emissions. *Nature Geoscience*, *11*, 38–43. https://doi.org/10.1038/s41561-017-0029-9

Lemos, G., Semedo, A., Hemer, M., Menendez, M., & Miranda, P. M. A. (2021). Remote climate change propagation across the oceans—The swell signature. *Environmental Research Letters*.

Lobeto, H., Menendez, M., & Losada, I. J. (2021). Future behavior of wind wave extremes due to climate change. *Scientific Reports*, *11*, 7869. https://doi.org/10.1038/s41598-021-86524-4

Marshall, A. G., Hemer, M. A., Hendon, H. H., & McInnes, K. L. (2018). Southern annular mode impacts on global ocean surface waves. *Ocean Modelling*, *129*, 58–74. https://doi.org/10.1016/j.ocemod.2018.07.007

Meehl, G. A., Senior, C. A., Eyring, V., Flato, G., Lamarque, J. F., Stouffer, R. J., et al. (2020). Context for interpreting equilibrium climate sensitivity and transient climate response from the CMIP6 Earth system models. *Science Advances*, *6*, eaba1981. https://doi.org/10.1126/sciadv.aba1981

Mentaschi, L., Vousdoukas, M. I., Voukouvalas, E., Dosio, A., & Feyen, L. (2017). Global changes of extreme coastal wave energy fluxes triggered by intensified teleconnection patterns. *Geophysical Research Letter*, *44*, 2416–2426. https://doi.org/10.1002/2016GL072488

Meucci, A., Young, I. R., Hemer, M., Kirezci, E., & Ranasinghe, R. (2020). Projected 21st century changes in extreme wind-wave events. *Science Advances*, *6*, 7295–7305. https://doi.org/10.1126/sciadv.aaz7295

Morim, J., Hemer, M., Wang, X. L., Cartwright, N., Trenham, C., Semedo, A., et al. (2019). Robustness and uncertainties in global multivariate wind-wave climate projections. *Nature Climate Change*, *9*(9), 711–718. https://doi.org/10.1038/s41558-019-0542-5

Morim, J., Trenham, C., Hemer, M., Wang, X. L., Mori, N., Casas-Prat, M., et al. (2020). A global ensemble of ocean wave climate projections from CMIP5-driven models. *Scientific Data*, *7*(1), 105. https://doi.org/10.1038/s41597-020-0446-2

O'Grady, J. G., Hemer, M. A., McInnes, K. L., Trenham, C. E., & Stephenson, A. G. (2021). Projected incremental changes to extreme wind-driven wave heights for the twenty-first century. *Scientific Reports*, *11*, 8826. https://doi.org/10.1038/s41598-021-87358-w

Patra, A., Min, S.-K., Kumar, P., & Wang, X. L. (2021). Changes in extreme ocean wave heights under 1.5°C, 2°C, and 3°C global warming. *Weather and Climate Extremes*, *33*, 100358. https://doi.org/10.1016/j.wace.2021.100358

Patra, A., Min, S.-K., & Seong, M.-G. (2020). Climate variability impacts on global extreme wave heights: Seasonal assessment using satellite data and ERA5 reanalysis. *Journal of Geophysical Research: Oceans*, *125*, e2020JC016754. https://doi.org/10.1029/2020JC016754

Reguero, B. G., Losada, I. J., & Méndez, F. J. (2015). A global wave power resource and its seasonal, interannual and long-term variability. *Applied Energy*, *148*, 366–380. https://doi.org/10.1016/j.apenergy.2015.03.114

Reguero, B. G., Losada, I. J., & Méndez, F. J. (2019). A recent increase in global wave power as a consequence of oceanic warming. *Nature Communications*, *10*, 205. https://doi.org/10.1038/s41467-018-08066-0

Semedo, A., Saetra, Ø., Rutgersson, A., Kahma, K. K., & Pettersson, H. (2009). Wave-induced wind in the marine boundary layer. *Journal of the Atmospheric Sciences*, *66*, 2256–2271. https://doi.org/10.1175/2009JAS3018.1

Sheng, W., & Li, H. (2017). A method for energy and resource assessment of waves in finite water depths. *Energies*, *10*(460), 1–17. https://doi.org/10.3390/en10040460

Sierra, J. P., & Casas-Prat, M. (2014). Analysis of potential impacts on coastal areas due to changes in wave conditions. *Climatic Change*, *124*, 861–876. https://doi.org/10.1007/s10584-014-1120-5

Smedman, A., Högström, U., Bergström, H., Rutgersson, A., Kahma, K. K., & Pettersson, H. (1999). A case study of air-sea interaction during swell conditions. *Journal of Geophysical Research*, *104*, 25833–25851. https://doi.org/10.1029/1999JC900213

Son, S.-W., Shin, J.-H., Park, H.-S., & Choi, J. (2021). The relationship between the zonal index and annular mode index in reanalysis and CMIP5 models. *Asia-Pacific Journal of Atmospheric Sciences*. https://doi.org/10.1007/s13143-021-00244-3

Sullivan, P. P., Edson, J. B., Hristov, T., & McWilliams, J. C. (2008). Large-eddy simulations and observations of atmospheric marine boundary layers above nonequilibrium surface waves. *Journal of the Atmospheric Sciences*, *65*, 1225–1245. https://doi.org/10.1175/2007JAS2427.1

Tucker, M. J., & Pitt, E. G. (2001). *Waves in ocean engineering*. Elsevier Science Ltd.

Wang, X. L., Feng, Y., & Swail, V. R. (2014). Changes in global ocean wave heights as projected using multimodel CMIP5 simulations. *Geophysical Research Letters*, *41*, 1026–1034. https://doi.org/10.1002/2013GL058650

Yang, S., & Oh, J. H. (2020). Effects of modes of climate variability on wave power during boreal summer in the western North Pacific. *Scientific Reports*, *10*(5187), 1–10. https://doi.org/10.1038/s41598-020-62138-0

Yim, B. Y., Min, H. S., & Kug, J. S. (2016). Inter-model diversity in jet stream changes and its relation to Arctic climate in CMIP5. *Climate Dynamics*, *47*, 235–248. https://doi.org/10.1007/s00382-015-2833-5

Young, I. R. (1999). Seasonal variability of the global ocean wind and wave climate. *International Journal of Climatology*, *19*(9), 931–950. https://doi.org/10.1002/(sici)1097-0088(199907)19:9<931::AID-JOC412>3.0.CO;2-O